Synthesis, Computational studies, DNA-binding and cytotoxicity of 4-Thiazolidonone-cyclopropyl hybrid

MD MUSHTAQUE (mush.chem@gmail.com)
AL-Falah University https://orcid.org/0000-0001-8662-2609

Fernando Avecilla
Universidade da Coruna

Mariyam Jahan
Al-Falah University

Irfan Ahmad
King Khalid University College of Science

Mohd Saeed
University of Hail College of Sciences

Gaffar Sarwar Zaman
King Khalid University College of Science

Kirtee Kamble
Savitribai Phule Shikshan Prasarak Mandal: Sinhgad Institutes

Subash S Pingale
Savitribai Phule Pune University

Research Article

Keywords: Synthesis, Stereochemistry, Ct-DNA binding, Computational studies, MTT-assay

Posted Date: May 14th, 2021

DOI: https://doi.org/10.21203/rs.3.rs-506702/v1

Abstract

A derivative of 4-Thiazolidinone derivative endowing cyclopropyl ring substituted at 3-nitrogen positioned was synthesized that was further evaluated against cancerous cell lines MCF-7. The structure of synthesized compound (6) was well characterized by different spectral techniques such as FT-IR, UV-Visible, ^{1}H-NMR, ^{13}C-NMR and mass spectrophotometer. X-ray single crystal structure and Computational study (DFT) study revealed that compound (6) adopted (2Z, 5Z)-*configuration*. Preliminary *In vitro* study suggested that compound (6) displayed moderate activity bearing IC_{50}(161.0 μM). The DNA binding studies (Ct-DNA) with compound (6) was performed. The study suggested that bound with DNA exhibiting binding constant K_b = 3.3 x 10^4 $LMol^{-1}$). Furthermore, the binding study was complemented by Molecular docking possessing

DNA binding studies (Ct-DNA) were performed. Final compound (6) exhibited moderate cytotoxicity effect (IC_{50} = 161.0 μM) and DNA binding ability (K_b = 3.3 x 10^4 $LMol^{-1}$). The experimental findings were completed by molecular docking study.

1. Introduction

Cancer is one of the notorious and gruesome diseases hovering around the globe. According the report published by International agency of Research on cancer (IARC) in 2012, 14.1 million new cases were estimated out of which 8.2 million were deaths. It was also reported that 19.3 cancer million cases would be confronted up to 2025[1]. However, 1.1 million cancer cases were estimated out of 184 countries contributing 7.8 % global cancer burden[1]. In spite of advancements in modern medical sciences, cancer is of the biggest challenges. There are many anti-cancer agents such as *cis*-platinum, doxorubicin, vincristine sulphate, etoposide etc but these drugs lack of selectivity and are associated with several effects sides. So, in order to curb these problems, there is an urgent need to develop new anti-cancer chemotherapeutics. For this purpose, heterocyclic compounds are important owing to the manifestation a wide spectrum of biological activities. To date, almost every drug in clinical applications contains one or more heterocyclic molecular scaffolds[2]. Among the heterocyclic compounds, 4-Thaiazolidinone endowing heteroatoms such as nitrogen, Oxygen and sulfur are five membered heterocyclic compounds which are known to exhibit a diverse range of pharmacological activities [3–6]. Drugs based on thiazolidinones core such as Pioglitazone, Troglitazone, Rosiglitazone Rivoglitazone, and Balaglitazone as shown in Chart1., have already been approved for the treatment of type diabetic and inflammatory conditions [7].

Considering versatile importance of thiazolidinone molecular scaffold, the scientists and researchers have explored the biological activities. The potent activities of 4-Thiazolidinone derivatives are anti-microbial[8–10], anti-cancer[11, 12] anti-viral[13], anti-convulsant[14], anti-inflammatory[15–17] and anti-amoebic[18]. We have a long-standing interest in the design and development of 4-thiazolidinones cores [3, 5, 18]. Our research group has earlier reported the stereochemistry and biological activity of 4-

ebic activity[18] and anti-cancer activity[4–6]. In quest of

developing a novel chemotherapeutic agent, our research group evaluated the compound against the cancerous cell lines. So, in the view of pharmacological significance, we herein report the synthesis, stereochemistry elucidation and pharmacological studies of 4-Thiazolidinone derivative bearing of cyclopropyl ring as a tail.

2. Results And Discussion

2.1. Chemistry

The synthesis of the lead compound (6) has been outlined in the scheme1, whose methodology has already been reported in our previous papers [5, 18]. The presented compound (6) was found to be stable at room temperature. The spectral techniques FT-IR, ^{1}H-NMR, ^{13}C-NMR and mass spectroscopy have been exploited to assign the structure of synthesized compounds. The final compound (6) was identified by X-ray single crystal structure as shown in Fig. 1.

The structures of the intermediate compounds (3 & 4) have already been reported in our previous work[5]. In this paper, the structure of the lead compound (6) has been explained with the help of spectral techniques. In FT-IR spectrum is used to detect the functional group which helps in identifying the presence of compound. In our investigated compound (6), the main identifying functional groups are (C = O) and (C = C) and the wavelengths of these functional groups were found to be at 1710.14 cm^{-1} and 1592.87 cm^{-1}. These bands showed the presence of compound (6). ^{1}H-NMR which is one of the most important techniques used to identify the organic and organometallic compounds. In our reported compound (6), the exocyclic alkenic proton (H-C = C-) resonated at high chemical shift δ 8.045 ppm which confirmed formation of compound (6). In the same way, the presence of characteristic chemical shifts resonated at 167.59 ppm and 148.58 ppm due to (-C = O) and (-C = C-) alkenic carbon in ^{13}C-NMR confirmed the formation of compound (6). Furthermore, in mass spectrometry, presence of $[M + H]^{+}$ peak at 351.0, $[M + 2H]^{+}$ at 352 and $[M + 3H]^{+}$ at 353.0 are the evidences of formation of compound (6). The solid-state structure of compound (6) was also confirmed by X-ray single crystal structure as shown in Figure (1).

2.2. X-ray single crystal structure

The ORTEP diagram of the compound (6) is shown in Figure (1). Selected bond distances and angles are given in Table (supplementary table (TS1). Phenyl ring of methoxyphenyl group and thiazolidin-4-one group are in the plane [mean deviation from planarity for C(1)-C(2)-C(3)-C(4)-C(5)-C(6)-C(7)-C(8)-C(9)-C(10)-N(1)-S(1)-O(1), 0.0813(10)Å]. Dihedral angle of this plane with cyclopropyl group is 62.98(5)º and with other phenylimino ring is 53.88(3)º. The π cloud around C(7) interacts strongly with delocalized π cloud of thiazolidin ring, $d_{C(7)-c1}$ = 3.379(1) Å [c1, C(8I)-C(9I)-C(10I)-S(1I)-N(1I)],[see Figure(2)], and forms antiparallel dimers between each two molecules in the crystal packing.

3. Computational Studies

3.1 Theoretical calculation on geometrical isomerism:

It is obvious that compound (6) bearing alkenic and exocylic nitrogen bonds may display four different configurations such as (2Z, 5Z), (2Z,5E), (2E,5Z) and (2E,5E). Among these most stable would be major product. So, in order to confirm the most stable the geometrical isomers of the compound (6), the DFT calculations were performed with Gaussian 09 software [19]. The structures of the various isomers i.e. (2Z, 5Z), (2Z, 5E), (2E,5Z) and (2E,5E) were energetically optimized at B3LYP/6-31G(d,p) level of theory and the results have been depicted in Table (1). In order to confirm that all the possible isomers have minima (zero point frequency), frequency calculations were performed. The geometry optimization of was performed at 6-311 + + G(d,p) basis set with B3LYP and M06-2X levels of theories. The energy obtained was exploited for further analysis. The optimized geometries have been visualized by UNIVIS software [20].

Table (1): Total electronic energy (E_{total}) of four different isomers of compound (6) and their relative energy (E_{rel}) with respect to (2Z, 5Z) isomer have been provided in the given table.

Isomers	Structures	B3LYP / 6-311++G(d,p)		M062X / 6-311++G(d,p)	
		E_{total} (au)	E_{rel} (kcal/mol)	E_{total} (au)	E_{rel} (kcal/mol)
(2*Z*,5*Z*)	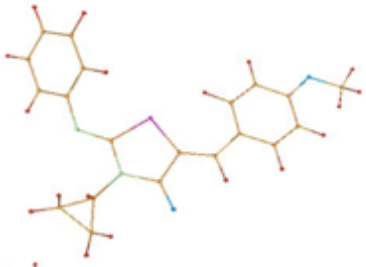	-1431.36812	0.0	-1430.91927	0.0
(2*Z*,5*E*)	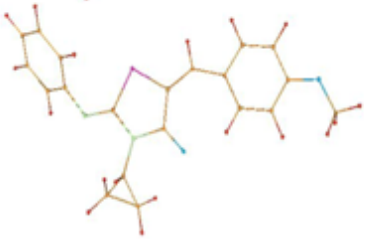	-1431.36092	4.52	-1430.91059	5.45
(2*E*,5*Z*)	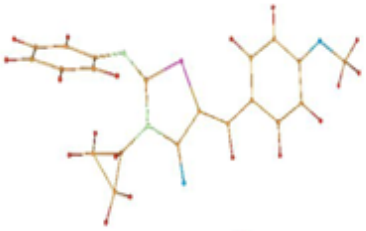	-1431.35947	5.43	-1430.91409	3.25
(2*E*,5*E*)	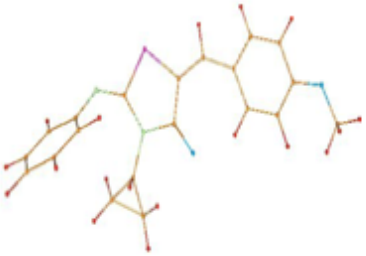	-1431.35199	10.12	-1430.90517	8.85

The results of the study suggested that compound (6) displayed most stable configuration in the form of (2*Z*, 5*Z*)-configuration. This computational study is completely in agreement with the experimental X-ray single crystal structure determination.

4. Pharmacological Activities

4.1 Cytotoxicity study

In order to know the anti-cancerous property of the compound (6), the cytotoxic study against cancerous cell lines (MCF-7) was evaluated by MTT-assay using vital dye. This dye is a chemical compound 3-(4,5-

m bromide. This dye is reduced by the succinate

dehydrogenase enzyme of mitochondrial living cells to produce water insoluble purple formazan crystals[21, 22] which can be measured spectrophotometrically after solubilization. It is well known fact that the quantity of formazan crystals produced is directly proportional to the number of active cells in the culture. Hence, MTT has long been exploited to measure the cell viability in cell proliferation and cytotoxicity [23, 24]. The compound (6) was evaluated against (MCF-7) cancerous cell lines for 48 hours treatment at the concentration range 0-320 µM as shown in Figure (5). The cytotoxic study revealed that compounds (6) displayed moderate activity (IC_{50} = 161.0 µM) which is considerable anti-cancer property.

4.2 DNA-binding study

In the prevalence of cancer DNA is quite important. Cell is multiply increased through the replication of DNA. So cell proliferation is prevented through DNA damage. In order to develop anti-cancer drug, DNA is regarded as one of the important targets. The evaluation of anti-cancer property of the newly synthesized Organic/organometallic compounds through DNA binding is quite important which bind with DNA in various ways[5, 25]. UV-Visible spectroscopy is one of the most commonly exploited techniques for the measurement of DNA- binding among all the available techniques[25]. The effectiveness of DNA-binding of the active compounds is explained by the change in absorption and wavelength. It is well known fact that non-covalent binding and covalent binding are characterized by bathochromism and hypochromism and hyperchromism[25]. The lowering of hypochromicity with no bathochromic shift describes the electrostatic interaction of a compound with DNA[26, 27]. From the Fig. 6 (a-b), it is evident that there are three significant peaks in the range of 200–405 nm, indicating interaction of compound (6) with Ct-DNA. It was found that on increment of the concentrations of the compound (6), hyperchromism was observed. The first electronic transition was found be at 402 nm due to n $\rightarrow\pi^*$ and the second transition was at 366 nm due to $\pi\rightarrow\pi^*$.The last electronic transition was observed at 230 nm is $\pi\rightarrow\pi^*$ due to benzene ring electrons. These transitions showed the considerable DNA-binding. From DNA-binding calculation, it was found that compound (6) exhibited binding constant (K_b) 3.3 x 10^4 L mol^{-1}. The lower value of K_b comparison to classical intercalations may be attributed to non-planarity in molecules[28] interestingly, same findings (grove binding) have been found in the docking studies. The DNA-binding studies have been presented in Fig. 6(a-b).

4.2 Molecular docking

Molecular docking is one of the best methods to select the hit compounds virtually. These days, it is very common and popular in the drug design and medicinal chemistry. The designed compounds are made to bind with a particular protein through which hit compound is scrutinized for the further process. With the help of molecular docking, active pocket and interacting residues are determined. In the present study, compound 6 was docked with DNA (PDBID: 1BNA) to complement Ct-DNA-binding outcomes. The DNA docking studies was performed by Auto Dock-vina [29, 30]using DNA dodecamers d(CGCGAATTCGCG)2 (PDB ID:1BNA). The study of the compound showed that compound (6) interacted with residues of the both the strands of DNA through polar and non-polar attractions as shown in Fig. 7(a-c). Similar result [illegible] dies. Besides, binding energy, is one of the physical

descriptors to compare the docking results, was found to have − 9.30 kcal/mol. The molecular docking as shown in Fig. 7(a-c) made five polar and non-polar interactions. The oxygen atoms of thiazolidinone ring of compound (6) form two hydrogen bonds with residues DC-10 & DC-9 of Chain A of DNA. However, the exocyclic nitrogen at position-2 formed three hydrogen bonds with the residues DA-17 and DA-18 of Chain B of DNA and with residue DC-9 of Chain A of DNA respectively. The 3D and 2D representations of compound 6 and DNA-interacting residues have been shown in Fig. 7(a-c).

5. Conclusion

We herein conclude on the basis of experimental and computational studies that the synthesized compound (6) adopted *(2Z, 5Z)-configuration*. Furthermore, the computational molecular docking study showed that compound 6 formed five hydrogen bonds bearing docking energy − 9.03 kcal/mol. Besides, the *in vitro* DNA-binding study revealed that binding constant of compound (6) was found to be K_b (3.3 x 10^4 $LMol^{-1}$) which is a significant binding constant. The MTT-assay evaluation for anti-cancer activity against cancerous cell lines depicted that compound 6 exhibited considerable IC_{50} value(IC_{50} = 161.0 µM).

6. Materials And Methods

All the required chemicals were purchased from Merck and Aldrich Chemical Company (USA). Precoated aluminium sheets (Silica gel 60 F254, Merck Germany) were used for thin-layer chromatography (TLC) and spots were visualized under UV light. Ct-DNA (as sodium salt) was obtained from SRL Pvt. Ltd, Mumbai, India. The concentrations of DNA were determined spectrometrically with an extinction coefficient of 6600 M^{-1} cm^{-1} at 258 nm. FT-IR spectra were recorded on Perkin Elmer model 1600 FT-IR RX1 spectrophotometer as KBr discs. ^{1}HNMR was recorded on Bruker Spectrospin DPX 300 MHz BrukerSpectrospin using $CDCl_3$ as a solvent and trimethylsilane (TMS) as an internal standard. Splitting patterns are designated as follows; s, singlet; d, doublet; m, multiplet. Chemical shift values are given in ppm. The ESI-MS was recorded on micrOTOF-Q II 10330 Electronspray ionization mass spectrometer (Bruker). X-ray data were collected on Bruker SMART Apex CCD diffractometer (SAI, Universidade da Coruña).

6.1 General procedure of synthesis of thiazolidinone derivative

(1.0 mmol)- (2Z)-3-cyclopropyl-2-(phenylimino)-1,3-thiazolidin-4-one(4), was dissolved in absolute ethanol in a round bottom flask and (1mmol) *p*-methoxy benzaldehyde was added followed by the addition of (1.15 mmol) hexahydropyridine to the reaction mixture. The reaction mixture was refluxed for 11–12 h. The progress of the reaction was monitored by TLC. After the completion of reaction of the yellow precipitated solid appeared and collected by filtration, washed with ethanol. The obtained product was recrystallized in chloroform at room temperature. The shining yellow crystal was obtained.

6.1.1(2Z, 5Z)-3-cyclopropyl-5-[(4-methoxyphenyl)methylidene]-2-(phenylimino)-1,3-thiazolidin-4-one: Yield: 85%; IR (λ_{max}) (cm^{-1}): 3013.21(Ar-H), 1710.14 (C = O), 1633.76(C = N),1592.87(C = C);^{1}H-NMR ($CDCl_3$)δ(ppm); 8.045 (s, 1H, H-C = C-), 7.391–7.280 (m, 3H, Ar-H), 7.171 (t, 1H, J = 4.2 Hz, Ar-H), 6.985 (d, 2H, J = 4.5 Hz, Ar-H), 6.933–6.830 (m, 3H, Ar-H),3.725(s, 3H, OCH_3), 2.928–2.884 (m, 1H, cyclopropyl proton), 1.089–0.944 (m, 4H, cyclopropyl); ^{13}C-NMR ($CDCl_3$)δ(ppm);167.59 (C = O), 153.42 (-C = N-), 148.58(-C = C-), 152.82, 129.33, 125.92, 124.77, 121.12, 116.05, 114.66, 112.08(Aromatic), 56.06(OCH_3), 25.92(-N-CH-), 7.97(cyclopropyl carbon-CH_2); Calc. mass: 350.0; exp.mass: $[M + H]^+$: 351.0 ; $[M + 2H]^+$: 352.0 ; $[M + 3H]^+$: 353.0

6.2 Cytotoxicity studies (MTT assay)

Cell culture

Breast cancer cell line (MCF-7) was obtained from NCCS (Pune India). Cell was cultured in Dulbecco's modified Eagle's medium (DMEM) with 10 % fetal bovine serum (heat inactivated), 100 units/mL penicillin, 100 µg/mL streptomycin, and 2.5 µg/mL amphotericin B, at 37 ^{0}C in a relative humidity 80 %, 5 % CO_2 [31].

MTT assay

The MTT assay is a standard colorimetric assay, in which mitochondrial activity is measured by splitting tetrazolium salts with mitochondrial dehydrogenases in viable cells only[32]. Cytotoxicity of compound (6) was evaluated through MTT (3-(4,5-dimethylthiazole-2-yl)-2,5-diphenyl tetrazolium bromide, M2128 Sigma Aldrich) assay on MCF-7. MTT is a validated assay for the in vitro cytotoxicity of any natural, synthetic compounds and extracts. The cell count 1.2 × 104 cells/well were seeded in 96 well plate (150 µL/well). After the overnight incubation, cells were treated with different concentration of compound (6) for 48 h. After the 48 h of treatment, the medium was remove and incubated with 20 µL of MTT solution (5 mg/mL in Phosphate saline buffer) for 4 hour. The formazan crystals were formed by mitochondrial enzyme reduction, finally solubilized in DMSO (150 µL/well) and absorbance was recorded at 570 nm through the Microplate reader (iMark, BIORAD, S/N 10321). Percent viability was defined as the relative absorbance of treated versus untreated control cells.

6.3 DNA-binding

The stock solution of disodium salt of Ct-DNA was prepared in tris-HCl buffer (pH 7.2–7.3) and stored at 4 ^{0}C temperature. Once prepared, the stock solution was used within 4 days. The concentration of the solution was determined spectrometrically. The ratio of absorbance at 260 and 280 (≥ 1.8) indicated that DNA was sufficiently free of protein. The concentration of DNA was measured using its extinction coefficient at 260 nm (6600 M^{-1} cm^{-1}) after dilutions. For the titration purpose, DNA stock solution was diluted using tris-HCl buffer. The compounds were dissolved in minimum amount of DMSO (1.6 x 10^{-4}M). UV-Vis absorption spectra were recorded after each addition of different concentrations of DNA. ıg varying concentrations (2.8–6.8 x 10^{-5} M) of DNA. The

intrinsic binding constant (K_b) was determined by Eq. (1), which was originally known as Benessi–Hilderbrand equation and further modified by Wolfe et. al.[33].

$$[DNA]/(\varepsilon_a - \varepsilon_f) = [DNA]/(\varepsilon_b - \varepsilon_f) + 1/K_b(\varepsilon_b - \varepsilon_f) \quad (1)$$

Where the apparent absorption coefficients ε_a, ε_f and ε_a correspond to A obs/[compounds], the extinction coefficient for the compounds, and the extinction coefficient for the compounds in the fully bound form. In plots of $[DNA]/(\varepsilon_a - \varepsilon_f)$ versus [DNA], K_b is given in the ratio of the slope to intercept.

6.3 DNA docking studies

Docking studies were performed at Intel(R) Core(TM) i3 CPU (2.3 GHz) with XP-based operating system (Windows 2010). 3D Structures of the compounds (6) was drawn by Marvin sketch and saved in pdb file format. The preparation of the compound was done by assigning Gastegier charges, merging non-polar hydrogens, and saving it in PDBQT file format using Auto-Dock Tools (ADT4.2)[29, 34, 35]. The X-ray crystal structure of DNA (PDB ID: 1BNA) was obtained from the Protein Data Bank [http://www.rcsb.org/pdb]. Using ADT 4.2, DNA was saved in PDB file format leaving heteroatoms (water). Gastegier charges were assigned to DNA and saved in PDBQT file format. Preparation of parameter files for grid and docking was done using ADT. Docking was performed with Auto Dock Vina 4.2[36] considering all the rotatable bonds of ligand (compound 3 and 4) as rotatable and receptor (DNA) as rigid[37]. A grid box of size 64 × 64 × 118 Å with 0.375Å spacing was used that included the whole DNA. The final structure of the docked complexes was drawn using PyMol[38] and 2D plot of docked complexes were constructed using Schrödinger visualizer (Maestro 10.5 trial version, Maestro, 2016).

6.4 X- Ray crystal structure determination

Three-dimensional X-ray data were collected on a Bruker Kappa Apex CCD diffractometer at low temperature by the φ-ωscan method. Reflections were measured from a hemisphere of data collected from frames, each of them covering 0.3º in ω.A total of 59758 for **6**, reflections measured were corrected for Lorentz and polarization effects and for absorption by multi-scan methods based on symmetry-equivalent and repeated reflections. Of the total, 4744 independent reflections exceeded the significance level ($|F|/\sigma|F|$) > 4.0. After data collection, an multi-scan absorption correction (SADABS)[39] was applied, and the structure was solved by direct methods and refined by full matrix least-squares on F^2 data using SHELX suite of programs [40]. Hydrogen atomswerelocated in difference Fourier map and left to refine freely, except for C(20), which were included in calculation position and refined in the riding mode. Refinements were done with allowance for thermal anisotropy of all non-hydrogen atoms. A final difference Fourier map showed no residual density outside: 0.403 and − 0.265 e.Å^{-3}.A weighting scheme $w = 1/[\sigma^2(F_o{}^2) + (0.052700\ P)^2 + 0.584300P]$ for **6**, where $P = (|F_o|^2 + 2|F_c|^2)/3$, was used in the latter stages of refinement. Further details of the crystal structure determination are given in Table (3). CCDC 2006786 contains the supplementary crystallographic data for the structure reported in this paper. These data can be obtained free of charge via http://www.ccdc.cam.ac.uk/conts/retrieving.html , or from the Cambridge Crystallographic Data Centre, 12 Union Road, Cambridge CB2 1EZ, UK; fax: (+ 44) 1223 336

033; or e-mail: deposit@ccdc.cam.ac.uk. Supplementary data associated with this article can be found, in the online version, at doi:

$.

Table (3): Crystal Data and Structure Refinement for the compound (2Z,5Z)-3-cyclopropyl-5-[(4-methoxyphenyl)methylidene]-2-(phenylimino)-1,3-thiazolidin-4-one(6)

Compound	6
Formula	$C_{20}\ H_{18}\ N_2\ O_2\ S$
Formula weight	350.42
T, *K*	100(2)
Wavelength, Å	0.71073
Crystal system	Monoclinic
Space group	$P2_1/n$
a/Å	11.9703(6)
b/Å	7.0182(4)
c/Å	20.4169(11)
β/º	93.083(2)
V/Å^3	1712.74(16)
Z	4
F_{000}	736
D_{calc}/g cm^{-3}	1.359
μ/mm^{-1}	0.205
θ/ (º)	3.37 to 31.64
R_{int}	0.0399
Crystal size/ mm^3	0.50 x 0.48 x 0.32
Goodness-of-fit on F^2	1.038
$R_1[I > 2\sigma(I)]$ [a]	0.0356
wR_2 (all data) [b]	0.1001
Largest differences peak and hole (eÅ^{-3})	0.403 and − 0.265

[a] $R_1 = S½çF_o÷ - êF_c÷½/S½F_o½$. [b] $wR_2 = \{S[w(½çF_o÷^2 - êF_c÷^2½)^2]½/S[w(F_o^2)^2]\}^{1/2}$

Declarations

Acknowledgement:

The authors, Dr. Md Mushtaque is thankful to Al-Falah University, Dhauj, Faridabad, Haryana, 121004, India for support and also Irfan Ahamd would like to acknowledge the support of the King Khalid University through a grant RCAMS/KKU/001/20 under the Research Center for Advanced Materials Science at King Khalid University, Saudia Arabia.

References

1. Saranath D, Khanna A (2014) Current status of cancer burden: global and Indian scenario. Biomed Res J 1(1):1–5
2. Gomtsyan A (2012) Heterocycles in drugs and drug discovery. Chem Heterocycl Compd 48(1):7–10
3. Mushtaque M, Avecilla F, Hafeez ZB, Rizvi MMA (2019) Synthesis, Characterization, Molecular Docking, and Anticancer Evaluation of 4-Thiazolidinone Analogues. J Heterocycl Chem 56(6):1794–1805
4. Mushtaque M, Avecilla F, Haque A, Perwez A, Khan MS, Rizvi MMA (2017) Experimental and theoretical studies of a pyrazole-thiazolidin-2, 4-di-one hybrid. J Mol Struct 1141:417–427
5. Mushtaque M, Avecilla F, Pingale SS, Kamble KM, Yab Z, Rizvi MMA (2017) Computational and experimental studies of 4-thiazolidinone-cyclopropyl hybrid. J Mol Liq 241:912–921
6. Mushtaque M, Avecilla F, Hafeez ZB, Jahan M, Khan MS, Rizvi MMA, Khan MS, Srivastava A, Mallik A, Verma S (2017) Synthesis, stereochemistry determination, pharmacological studies and quantum chemical analyses of bisthiazolidinone derivative. J Mol Struct 1127:99–113
7. Montoya J, Giraldo GA, Sánchez LT (2019) Efecto de Diferentes Aditivos sobre el Comportamiento Reológico de Masas de Harina de Plátano Dominico Hartón (Musa paradisiaca L.). Información tecnológica 30(4):3–12
8. Fesatidou M, Zagaliotis P, Camoutsis C, Petrou A, Eleftheriou P, Tratrat C, Haroun M, Geronikaki A, Ciric A, Sokovic M (2018) 5-Adamantan thiadiazole-based thiazolidinones as antimicrobial agents. Design, synthesis, molecular docking and evaluation. Bioorg Med Chem 26(16):4664–4676
9. Abo-Ashour MF, Eldehna WM, George RF, Abdel-Aziz MM, Elaasser MM, Gawad NMA, Gupta A, Bhakta S (2018) S.M. Abou-Seri, Novel indole-thiazolidinone conjugates: Design, synthesis and whole-cell phenotypic evaluation as a novel class of antimicrobial agents. Eur J Med Chem 160:49–60
10. Angapelly S, PS R, SunithaRani R, Kumar CG, Kamal A, Arifuddin M (2017) Ultrasound assisted, VOSO4 catalyzed synthesis of 4-thiazolidinones: Antimicrobial evaluation of indazole-4-thiazolidinone derivatives. Tetrahedron Lett 58(49):4632–4637
11. Holota S, Kryshchyshyn A, Derkach H, Trufin Y, Demchuk I, Gzella A, Grellier P, Lesyk R (2019) Synthesis of 5-enamine-4-thiazolidinone derivatives with trypanocidal and anticancer activity. Bioorganic chemistry 86:126–136
12. Szychowski KA, Leja ML, Kaminskyy DV, Binduga UE, Pinyazhko R, Lesyk RB, Gmiński J (2017) Study of novel anticancer 4-thiazolidinone derivatives. Chemico-Biol Interact 262:46–56

13. Cihan-Üstündağ G, Gürsoy E, Naesens L, Ulusoy-Güzeldemirci N, Çapan G (2016) Synthesis and antiviral properties of novel indole-based thiosemicarbazides and 4-thiazolidinones. Bioorg Med Chem 24(2):240–246
14. Jain AK, Vaidya A, Ravichandran V, Kashaw SK, Agrawal RK (2012) Recent developments and biological activities of thiazolidinone derivatives: A review. Bioorg Med Chem 20(11):3378–3395
15. Abdellatif KR, Abdelgawad MA, Elshemy HA, Alsayed SS (2016) Design, synthesis and biological screening of new 4-thiazolidinone derivatives with promising COX-2 selectivity, anti-inflammatory activity and gastric safety profile. Bioorganic chemistry 64:1–12
16. Tageldin GN, Fahmy SM, Ashour HM, Khalil MA, Nassra RA, Labouta IM (2018) Design, synthesis and evaluation of some pyrazolo [3, 4-d] pyrimidine derivatives bearing thiazolidinone moiety as anti-inflammatory agents. Bioorganic chemistry 80:164–173
17. Omar YM, Abdu-Allah HH, Abdel-Moty SG, Synthesis, biological evaluation and docking study of 1, 3, 4-thiadiazole-thiazolidinone hybrids as anti-inflammatory agents with dual inhibition of COX-2 and 15-LOX, Bioorganic chemistry 80 (2018) 461–471
18. Mushtaque M, Avecilla F, Azam A (2012) Synthesis, characterization and structure optimization of a series of thiazolidinone derivatives as Entamoeba histolytica inhibitors. Eur J Med Chem 55:439–448
19. Frisch M, Clemente F, G 09, Revision, A 01, MJ Frisch, Trucks GW, Schlegel HB, Scuseria GE, Robb MA, Cheeseman JR, Scalmani G, Barone V, Mennucci B, Petersson GA, Nakatsuji H, Caricato M, Li X, Hratchian HP, AF Izmaylov, J. Bloino, G. Zhe
20. Limaye AC, Gadre SR (2001) UNIVIS-2000: an indigenously developed comprehensive visualization package. Curr Sci(India) 80:1296–1300
21. Thom SM, Horobin R, Seidler E, Barer M (1993) Factors affecting the selection and use of tetrazolium salts as cytochemical indicators of microbial viability and activity. J Appl Bacteriol 74(4):433–443
22. Kim SR, Park MJ, Lee MK, Sung SH, Park EJ, Kim J, Kim SY, Oh TH, Markelonis GJ, Kim YC (2002) Flavonoids of Inula britannica protect cultured cortical cells from necrotic cell death induced by glutamate. Free Radic Biol Med 32(7):596–604
23. Kim S-H, Zo J-H, Kim M-A, Hwang K-K, Chae I-H, Kim H-S, Kim C-H, Sohn D-W, Oh B-H, Lee M-M (2003) Naringin suppresses the mitogenic effect of lysophosphatidylcholine on vascular smooth muscle cells. Nutrition research 23(12):1671–1683
24. Lin H-Y, Juan S-H, Shen S-C, Hsu F-L, Chen Y-C (2003) Inhibition of lipopolysaccharide-induced nitric oxide production by flavonoids in RAW264. 7 macrophages involves heme oxygenase-1. Biochem Pharmacol 66(9):1821–1832
25. Zhang G, Hu X, Fu P (2012) Spectroscopic studies on the interaction between carbaryl and calf thymus DNA with the use of ethidium bromide as a fluorescence probe. J Photochem Photobiol B 108:53–61
26. Xu X, Wang D, Sun X, Zeng S, Li L, Sun D (2009) Thermodynamic and spectrographic studies on the interaction of 5-fluorouracil and tegafur. Thermochimica acta 493(1–2):30–36

27. Patel MN, Parmar PA, Gandhi DS, Patidar AP (2012) DNA interactions and cytotoxic studies of cis-platin analogues of substituted 2, 2'-bipyridines. Spectrochim Acta Part A Mol Biomol Spectrosc 97:54–59
28. Long EC, Barton JK (1990) On demonstrating DNA intercalation. Acc Chem Res 23(9):271–273
29. Morris GM, Goodsell DS, Halliday RS, Huey R, Hart WE, Belew RK, Olson AJ (1998) Automated docking using a Lamarckian genetic algorithm and an empirical binding free energy function. J Comput Chem 19(14):1639–1662
30. Kitchen D, Decornez H, Furr J, Bajorath J (2004) Structure-based virtual screening and lead optimization: methods and applications. Nature Rev Drug Discov 3:935–949
31. Gupta MK, Neelakantan T, Sanghamitra M, Tyagi RK, Dinda A, Maulik S, Mukhopadhyay CK, Goswami SK (2006) An assessment of the role of reactive oxygen species and redox signaling in norepinephrine-induced apoptosis and hypertrophy of H9c2 cardiac myoblasts. Antioxid Redox Signal 8(5–6):1081–1093
32. Mosdam T (1983) Rapid colorimetric assay for cellular growth and survival: application to proliferation and cytotoxic assay. J Immunol Methods 65:55–63
33. Wolfe A, George H, Shimer J (1987) Thomas Meehan, Polycyclic aromatic hydrocarbons physically intercalate into duplex regions of denatured DNA. Biochemistry 26:6392–6396
34. Autodock A, Morris GM, Goodsell DS, Halliday RS, Huey R, Hart WE, Belew RK, Olson AJ, Automated Docking Using a Lamarckian Genetic Algorithm and an Empirical Binding Free Energy Function, (1998)
35. Huey R, Morris GM, Olson AJ, Goodsell DS (2007) A semiempirical free energy force field with charge-based desolvation. J Comput Chem 28(6):1145–1152
36. Vina A (2010) Improving the speed and accuracy of docking with a new scoring function, efficient optimization, and multithreading Trott, Oleg; Olson, Arthur J. J Comput Chem 31(2):455–461
37. Sanner MF (1999) Python: a programming language for software integration and development. J Mol Graph Model 17(1):57–61
38. DeLano WL, PyMOL, 2002
39. Sheldrick G (2001) SADABS version 2.10; University of Göttingen. There is no corresponding record for this reference.[Google Scholar]
40. Sheldrick G, SHELXL-2016/6: Program for Crystal Structure Determination, University of Göttingen, Göttingen, Germany (2016)

Supplementary Information

Supplementary Table S1 was not provided with this version of the manuscript.

Figures

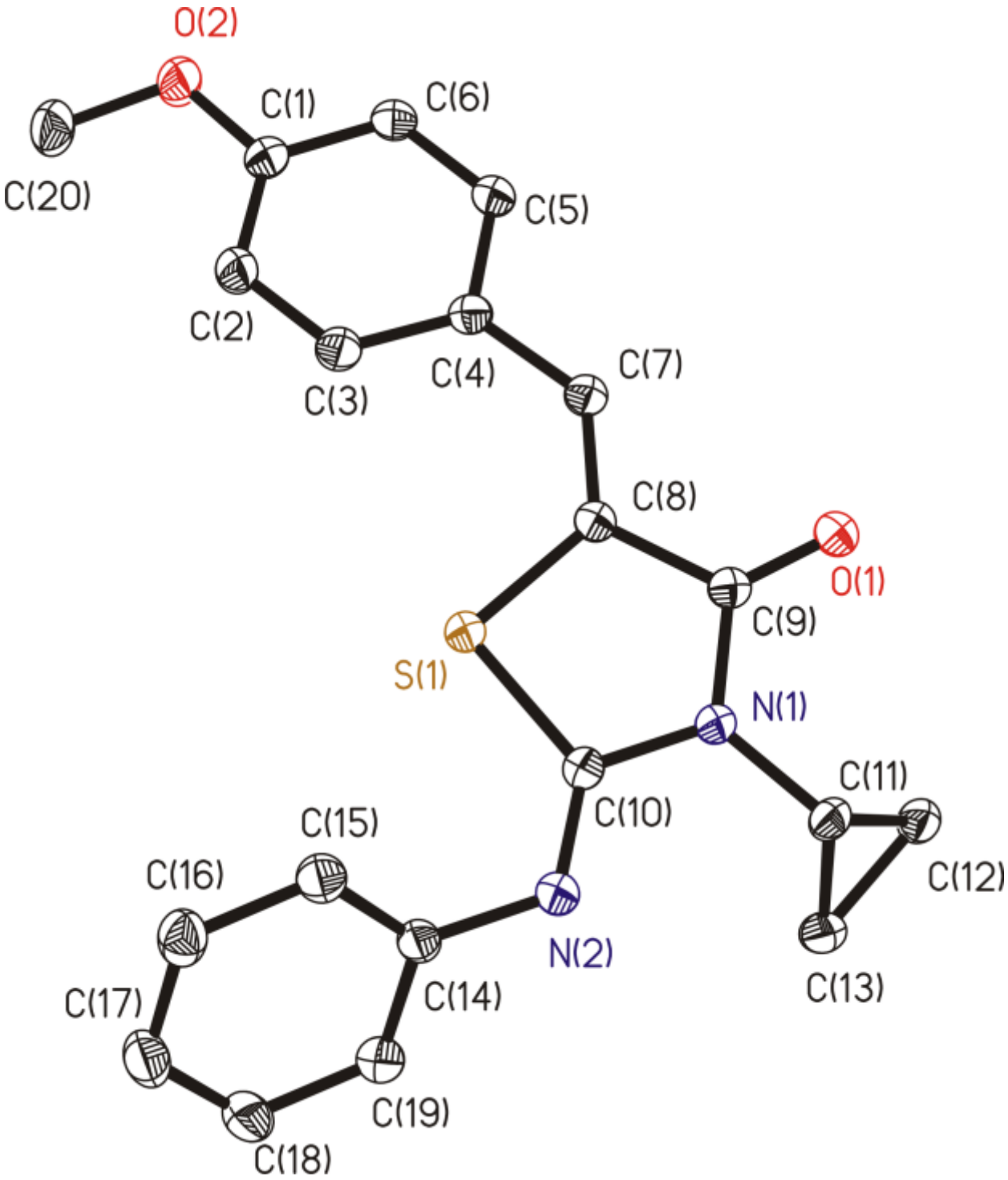

Figure 1

ORTEP for the compound (6). Hydrogen atoms are omitted by clarity. All the non-hydrogen atoms are presented by their 50% probability ellipsoids.

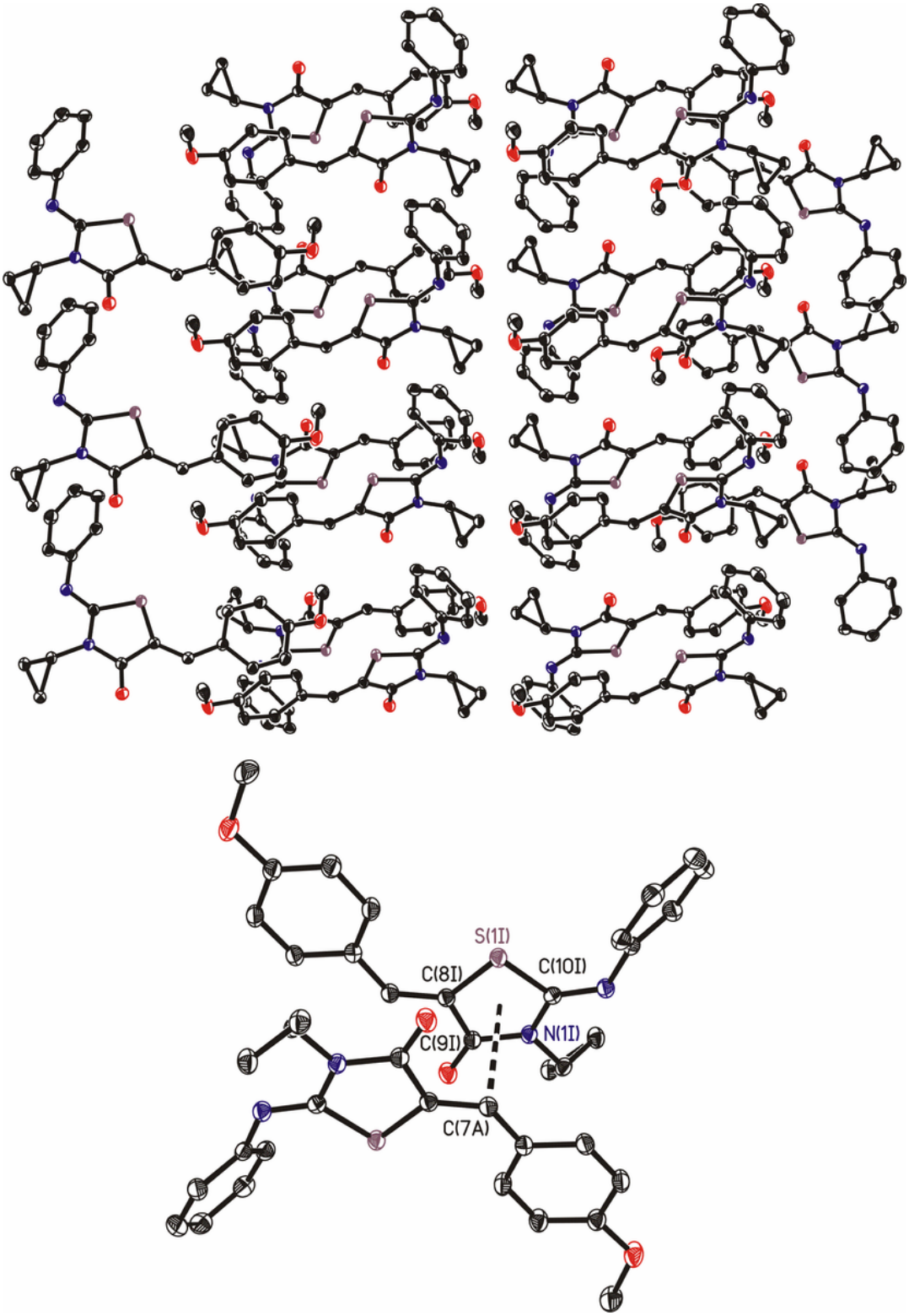

Figure 2

Crystal packing in the compound (6) is shown up. Drawing of two antiparallel molecules present in the crystal packing, down, which interact through π clouds.

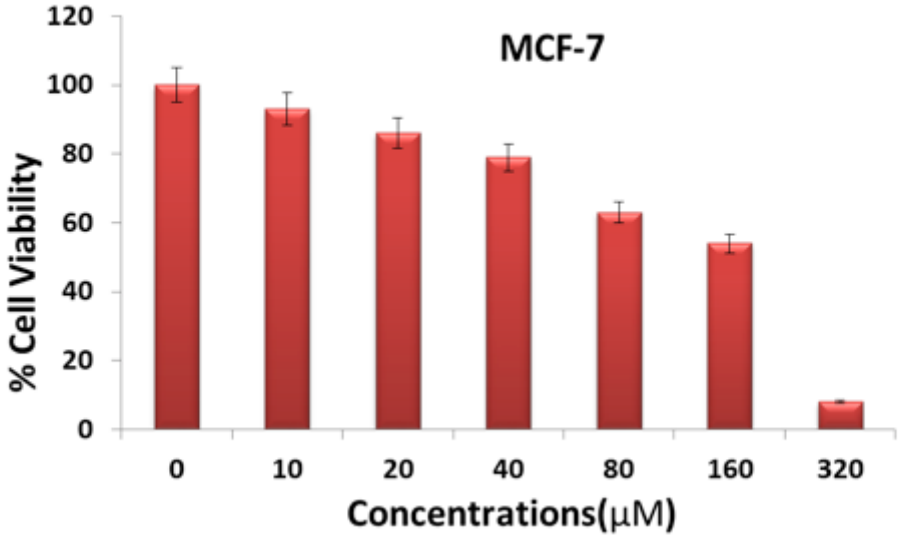

Figure 3

(Manuscript Figure 5) Percentage cells viability of compound (6) against MCF-7 cells at the concentration range 10-320 (μM).

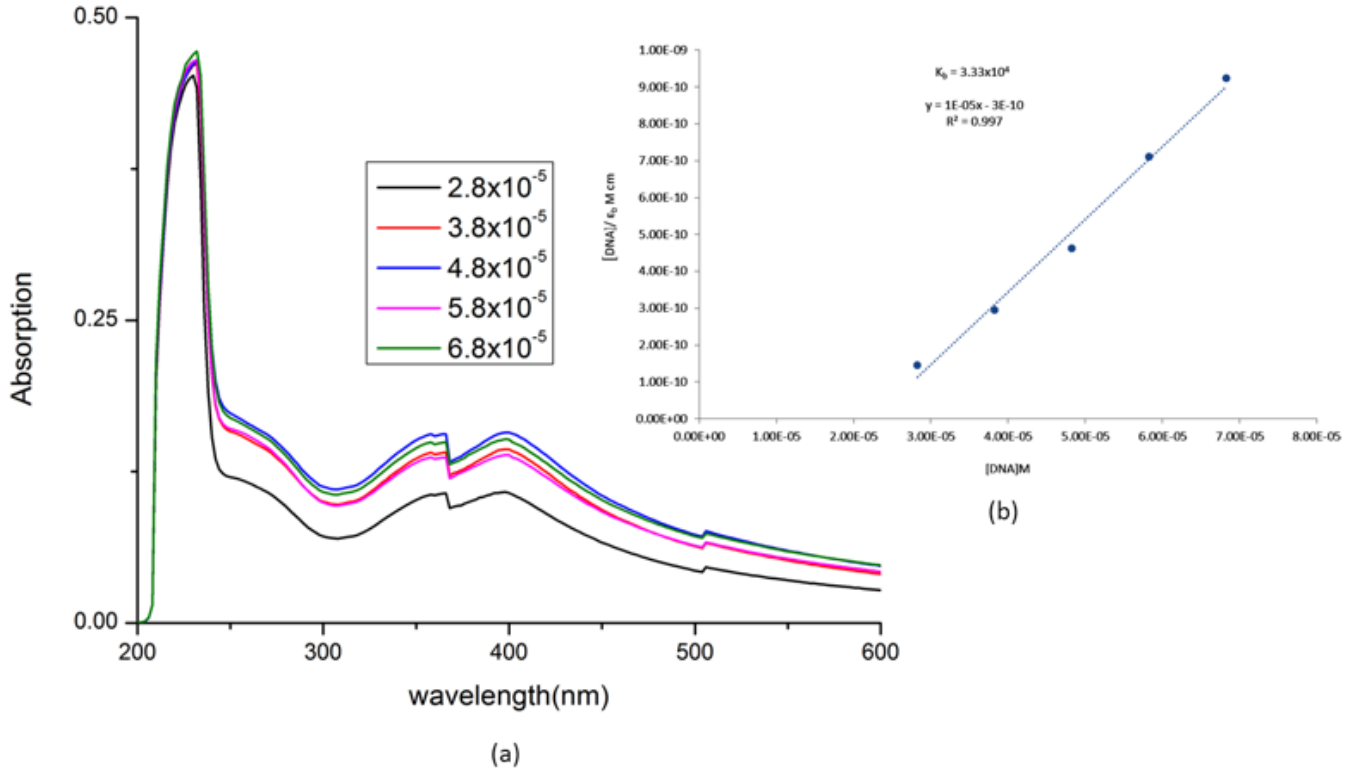

Figure 4

(Manuscript FIgure 6) (a-b): Absorption spectra of compound (6) and DNA binding spectra of compound in the presence of increasing concentration of Ct-DNA. Inset: plots of [DNA]/(□a− □f) (M2 cm-1) versus [DNA] for thetitration of CT DNA with compounds. Experimental data points; full lines, linear fitting of the data. (Compound 6) 1.6 x 10-4 M, [DNA] 2.8-6.8 x 10-5 M.

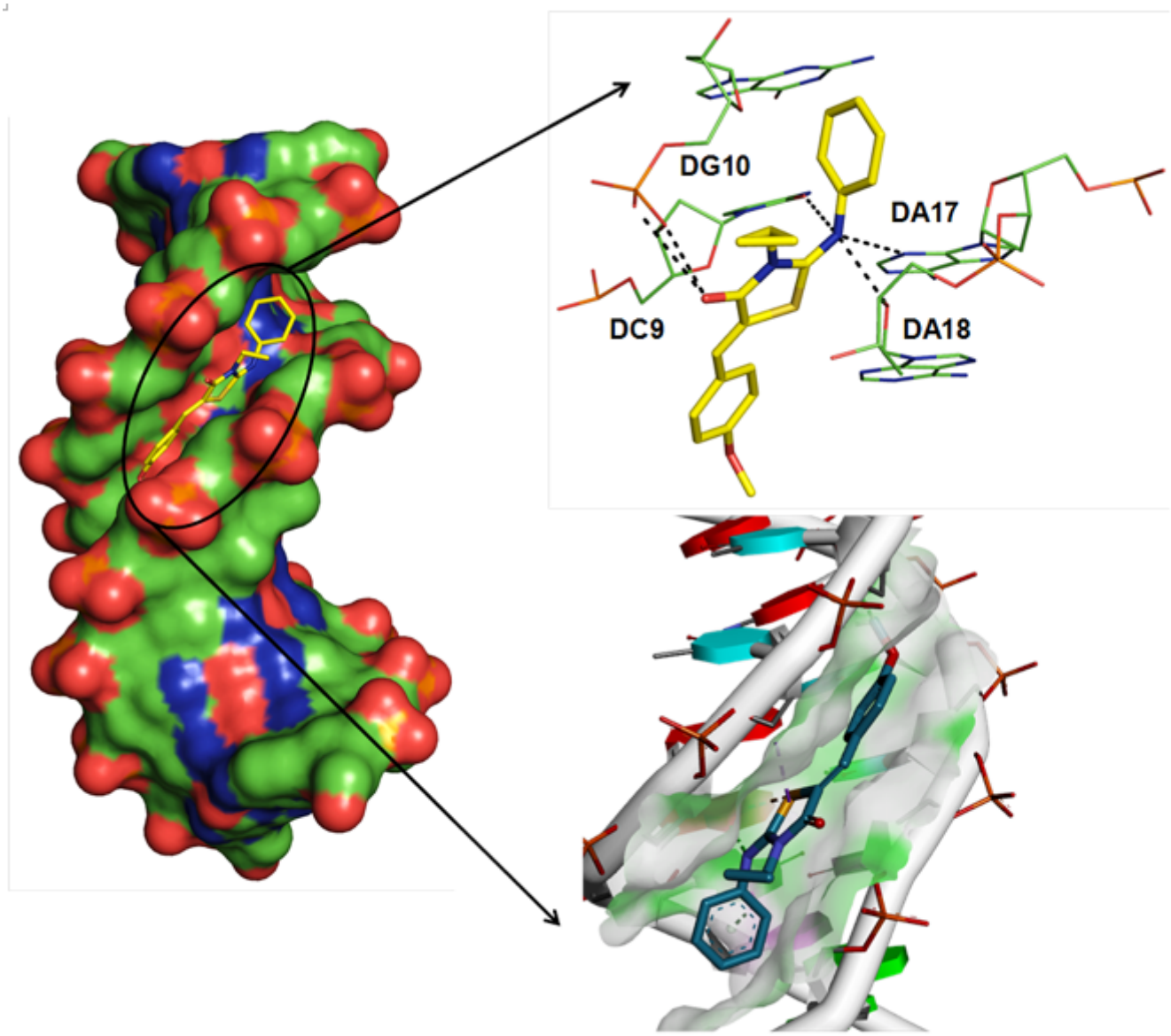

Figure 5

(Manuscript Figure 7) (a-c): 3D-presentation of molecular docking of compound (6) with known receptor (PDBID: 1BNA). (a) Represents the 3D-surface presentation (b) represents the 2D-cartoon presentation(c) represents the interaction of compound(c) with the residues of DNA (PDBID: 1BNA)

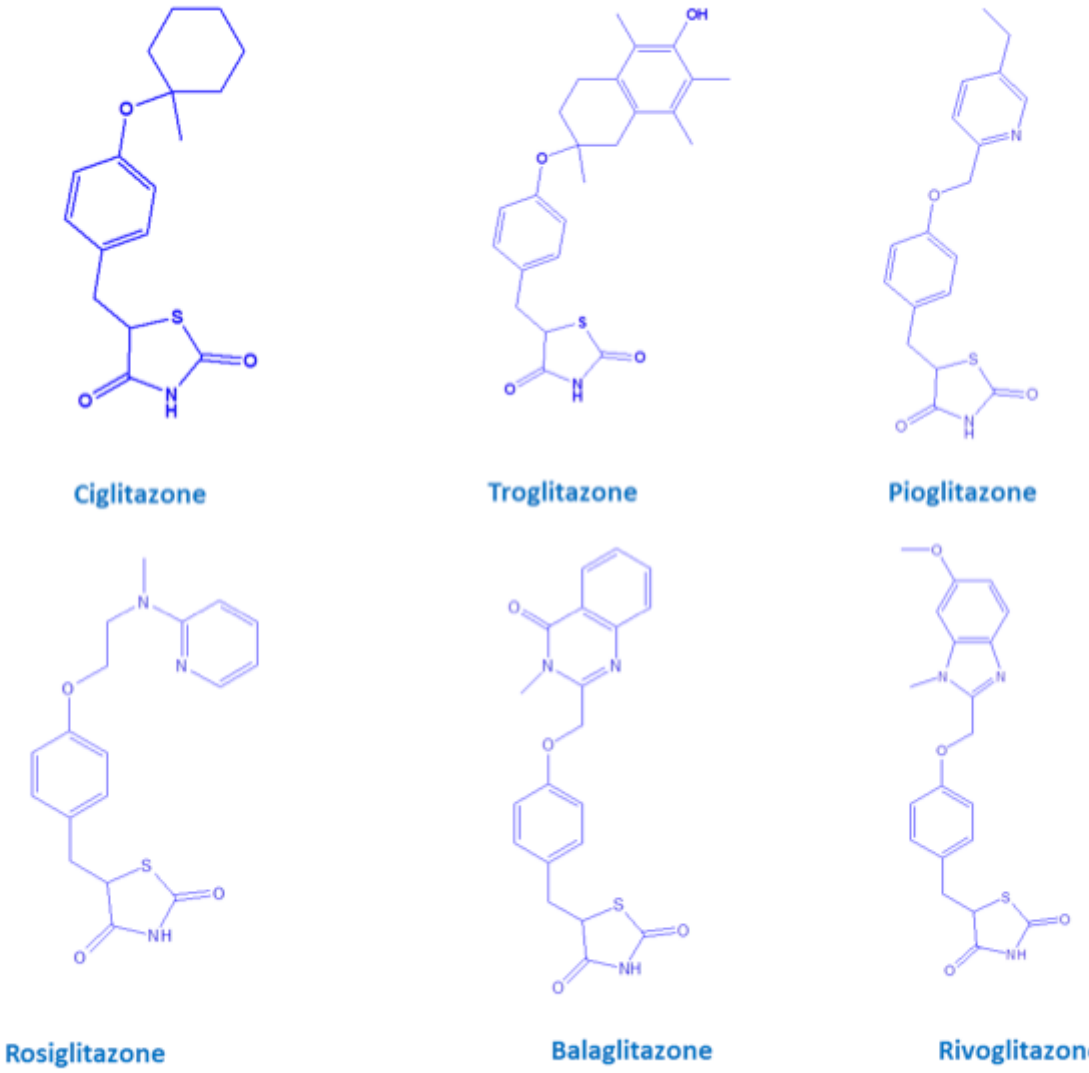

Figure 6

Chart 1: Some thiazolidinones based pharmaceutical agents.

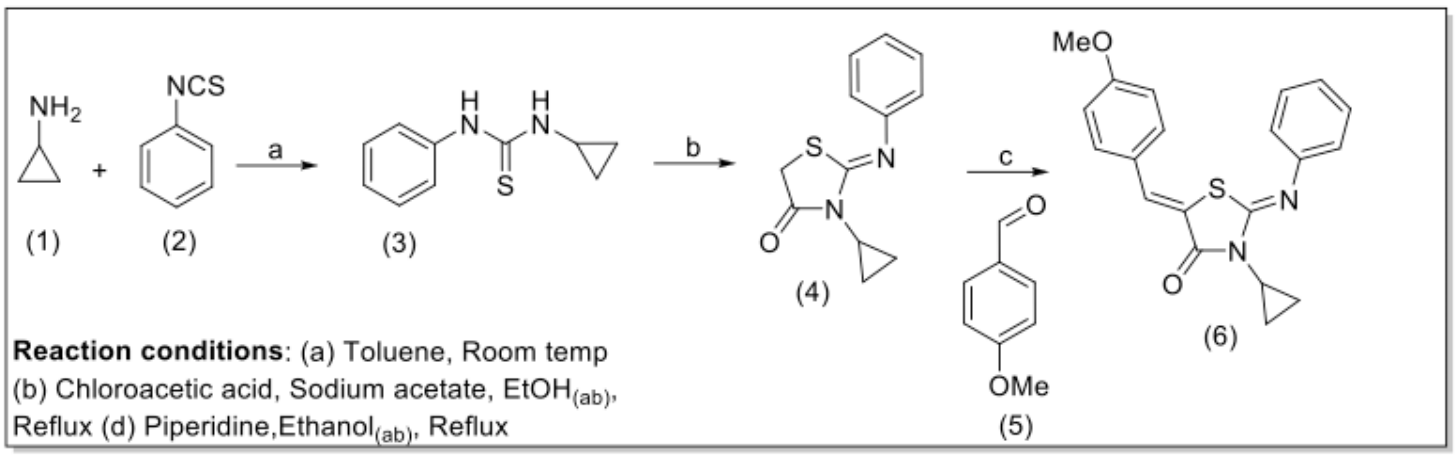

Figure 7

Scheme 1: Synthetic scheme for 4-Thiazolidinone derivative (6)

Supplementary Files

This is a list of supplementary files associated with this preprint. Click to download.

- Onlinefloatimage1.png